Research Article

Journal of Environmental Nanotechnology

Synthesis and Characterization of Ag-decorated TiO_2 Nanoparticles for Photocatalytic Application

K. Balachandran*, G. Vijayakumar, S. Mageswari, A. Preethi, M.S. Viswak Senan

Research Centre, Department of Chemistry, Vivekanandha College of Engineering for Women, Namakkal, TN, India

Received: 12.11.2021 Accepted: 21.11.2021 Published: 30-12-2021

*balanano06@gmail.com

ABSTRACT

TiO_2 nanoparticles and Ag-doped TiO_2 nanocomposites (Ag-TiO_2) were synthesized by the Sol-Gel process using titanium tetra isopropoxide as TiO_2 and $AgNO_3$ as Ag precursors, respectively. The synthesized nanocomposites were characterized by XRD, SEM, TEM, FT-IR and UV-Visible analyses. The XRD results show that Ag-doping increases the grain size from 22 nm to 36 nm. From the UV-Visible spectra, the redshift in absorbance was observed, which indicates the increase in grain size and reduction in the bandgap. The TEM analysis shows that all the particles are exhibited in the nanometer range. The synthesized nanoparticles show good photocatalytic activity and they decompose the methyl orange dye within 5 hours.

Keywords: Ag-TiO_2; Methyl Orange; Photocatalyst; TEM; TiO_2.

1. INTRODUCTION

In this present century, the synthesis of nanomaterials is much sought-after, owing to its extensive applications. Particularly, semiconducting metal oxide has gained more attention due to its merits when compared to other materials. Especially, semiconducting materials such as TiO_2 have attracted more curiosity in photocatalysts, photovoltaic cells, water purification, gas sensors and biomedical devices owing to their uniqueness, different band structure, good mechanical behavior and chemical stability (Fukuda *et al.* 2004; Wang *et al.* 2008). TiO_2-based material has been investigated due to its non-toxicity, high stability and inexpensiveness (Liu *et al.* 2010) and also finding various synthesis routes. Wet chemical synthesis is one of the fine-tuned methods because of its fascinating benefits that can be cited when utilizing the Sol-Gel method:

(1) better control of structure and particle size
(2) better homogeneity in terms of molecular level
(3) selective heating with minimal loss of heat and
(4) relatively compact apparatus.

TiO_2 materials have gained attention from semiconducting researchers worldwide due to their special tunable properties and corresponding applications. Moreover, TiO_2 has been widely applied as a photocatalyst due to its high reactivity, strong oxidizing power for the decomposition of organic pollutants, non-toxic, chemical inertness, photo-stability, environment-friendliness, and low cost (Fox *et al.* 1993; Burns *et al.* 2004; Guo *et al.* 2012; Rajamanickam *et al.* 2015). Typically, TiO_2 exhibits rutile, brookite and anatase in three phases. Rapid synthesis of TiO_2 based nanomaterials with controllable nanostructure with doping (Ag/La/Graphene) is possible.

The Sol-Gel method was used in this work to synthesize TiO_2 nanoparticles. We further generated and optimized Ag-TiO_2 nanocomposites with different compositions and Ag concentrations ranging from 2.5 to 10 % by weight. The size and form of the nanoparticles have also been influenced. The impact of the usefulness of the photocatalytic activity of the catalyst was analyzed; other ways for nanoparticle production would be examined further. X-ray diffractometry (XRD), scanning transmission electron microscopy (STEM) and energy-dispersive X-ray spectroscopy were used to analyze the produced nanoparticles (EDX) and ultraviolet-visible spectroscopy (UV-Vis) and Fourier Transformation Infrared spectroscopy (FTIR) for photocatalytic studies. The nanoparticles and nanocomposites were then tested for their ability to decompose methyl orange dye over a range of time intervals and concentrations. Under UV light, the catalytic degradation performance of pure TiO_2 and Ag-TiO_2 were evaluated.

2. MATERIALS AND METHODS

2.1 Materials

All reagents used were of analytical grade purity and were procured from Merck Chemical Reagent Co., Ltd., India.

2.2 Synthesis of TiO_2 Nanoparticles

Titanium tetra isopropoxide (TTIP) was used as a precursor, Hydrochloric acid (HCl) as a peptizing agent and ethanol as a solvent medium. HCl was mixed with ethanol and was stirred for a few minutes. To this mixture, TTIP was added in the ratio of 1:4:2 and the stirring was continued for 1 hour at room temperature. Then 100 ml of distilled water was added, the temperature was raised to 50 ºC and stirred for 3 hours until the solution changed into a colorless gel. The high-viscous gel was dried at room temperature to a fine powder. The resulting powder was heated at 120 ºC for 1 hour in a hot air oven. Finally, the colorless powder was calcined at 400 ºC for 2 hours.

2.3 Synthesis of Ag-doped TiO_2 Nanoparticles

The TiO_2 solution was prepared by the above-said method. $AgNO_3$ solutions at various concentrations (2.5 -10%) were added to this solution to form Ag-TiO_2 composites.

The concentration of silver nitrate solution was varied from 2.5 % to 10 % in steps of 2.5%. The total concentration of the solution was maintained at 0.1 mol/litre. Silver nitrate solution was added to the above solution with (Ag/Ti) nominal volume proportions 2.5, 5, 7.5 and 10 % and stirring was continued for 3 hours to form Ag-TiO_2 nanocomposites. The fine residue was rinsed with deionized water and dried for 1 hour at 120 ºC. The powder was then calcined for 2 hours at 400 ºC.

2.4 Characterization of Synthesized TiO_2 Nanoparticles and Ag-TiO_2 Nanocomposites

The optical properties of TiO_2 nanoparticles and Ag-TiO_2 nanocomposites were characterized by UV–Visible spectroscopy (Carry 5000 UV–Vis-NIR spectrophotometer, Varian, USA). The crystalline structure of synthesized TiO_2 nanoparticles and Ag-TiO_2 nanocomposites were analyzed using D8 Advance X-ray diffraction meter (Bruker AXS, Germany) at room temperature, operating at 30 kV and 30 mA, using Cu Ka radiation (k = 0.15406 nm), and Scherrer's formula was used to calculate crystal size. The surface morphology of synthesized TiO_2 nanoparticles and Ag-TiO_2 nanocomposites were characterized using a scanning electron microscope (SEM) (Model JSM 6390LV, JOEL, USA). The nanoparticles and composites were viewed through a transmission electron microscope (TEM) (JEOL-TEM 2100) at high magnification and exact particle size was predicated.

2.5 Measurement of Photocatalytic Activity

Experiments were performed with an aqueous solution of methyl orange with TiO_2 nanoparticles and Ag-TiO_2 nanocomposites under sunlight radiation. All the reactions were carried out under pH 9. TiO_2/methyl orange and Ag-TiO_2 suspensions were prepared for 10 mg L1 of methyl orange. Prior to sunlight radiation (5 h irradiation), the suspensions were stirred for 30 min to allow for dye adsorption onto the nanoparticle surface. 10 mL of the sample was collected and centrifuged to remove nanoparticles and the clear solution was carefully transferred into a quartz cuvette and the absorption was evaluated by UV–Vis spectrometer (kmax). The dye adsorbed after equilibrium time was separated by centrifugation and the quantity of dye adsorbed was determined by employing a UV–Visible spectrophotometer.

3. RESULTS AND DISCUSSION

3.1 SEM and EDAX analysis

TiO_2 and Ag-TiO_2 nanoparticles were synthesized by Sol-Gel synthesis strategy in this research work. SEM and TEM analysis analyzed the morphology and microstructure of the nanoparticles. The synthesized TiO_2 and Ag-TiO_2 were characterized by SEM analysis, which revealed the spherical shape of the particles with a diameter of nanosize to maximum 3.30 μm diameter with a few agglomerations (Fig. 1). It was clearly shown in the figure (Fig. 1a and 1b) with a different magnification of TiO_2. Fig. 1c and 1d images revealed the presence of silver nanoparticles to a maximum of 1.54 μm with spherically-grown agglomerated micro and few nanosize particles. The Ag-TiO_2 morphology shows a spongy-like appearance with some dense and smaller grains size particles than pure TiO_2 over there. Further, Fig. 1e shows the EDAX analysis that the average atomic percentage of nano-Ag is around 10% and with TiO_2 inter lattice, thus indicating the Ag^+ ions were inbuilt in TiO_2 crystal lattice.

3.2 TEM Analysis

Further evidence of nanostructure can be clearly identified by transmission electron microscopy (TEM), which is displayed in Fig 2. (a-b). The synthesized pure TiO_2 and silver-doped TiO_2 show several nanometers maximum 50 nm and 20 nm, respectively. As synthesized Ag-TiO_2 formation of the particles has differed with respect to silver ion presence. Pure TiO_2 was agglomerated with a mixture of spherical, dendritic, and a few lower-like shapes compared to Ag-TiO_2. The average diameters of Ag-TiO_2 as-synthesized nanoparticles are around 20 nm than pure TiO_2 images, which is reliable with the SEM images.

3.3 XRD Analysis

Fig. 3 (a and b) shows XRD patterns of the two synthesized samples, clearly confirming strong diffraction peaks at 25.6°, 36.2°, 41.2°, 48.4° and 62.57°,

which correspond to the crystal planes of (1 0 1), (0 0 4), (2 0 0) and (2 0 4), etc. of the standard card of anatase-type TiO_2,(PDF=21-1272) (Jiang *et al.* 2011). No such characteristic peaks from the 211 crystal plane of brookite as well as the 110 crystal plane of rutile pointed out, the appearance of anatase phase crystals, and crystalline size is 22 nm. The characteristic peak of the 111 crystal plane of Ag was noted at 25.6°, which was covered by strong diffraction peaks in the vicinity of the 101 crystal plane of anatase TiO_2 at 25.6. It revealed that the doping of silver ions could increase the particle size of TiO_2 up to 36 nm has a significant quantum size effect so that Ag-TiO_2 can provide better photocatalytic behavior (Almquist *et al.* 2002).

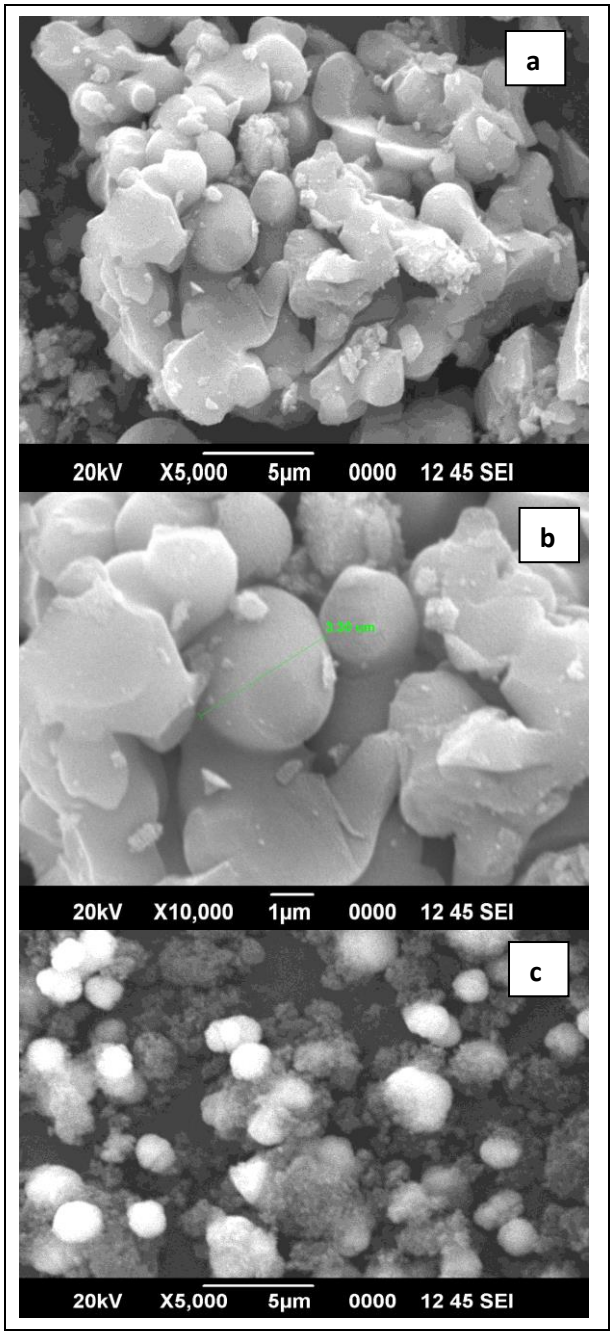

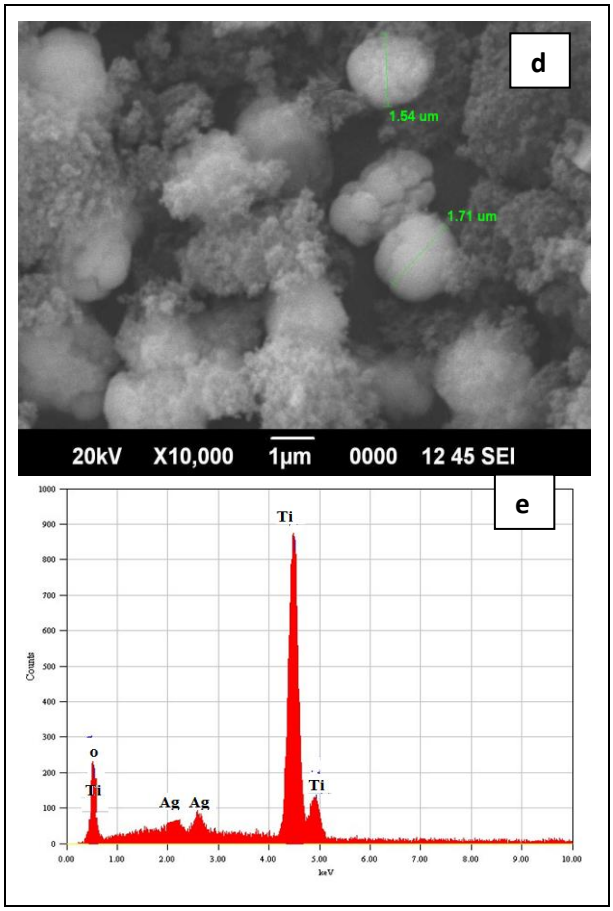

Fig. 1. (a, b) SEM images of pure TiO_2 and (c, d) images of Ag-TiO_2 nanoparticles (e) EDAX analysis of Ag-TiO_2 nanoparticles

Further evidence, in the case of Ag-TiO_2 sample, shows sharp and little broad peak indicates that crystalline, as well as nanostructure, has built well, which has good agreement with the results are showed nanoparticle. Therefore, rutile and brookite phases have not been detected (Sahu *et al.*, 2011). Further, we compared the pure TiO_2 and Ag-TiO_2 samples only peak position at 36.1°, which indicates the Ag+ ion dopped in the TiO_2 structure corresponding plan (111). Hence, the anatase phase possesses a higher effective photocatalyst character than the rutile phase titania because it has a more existing vacancy and defect (Abdul Gafoor *et al.*, 2012). Scherrer's equation calculated the crystallite size from the full-width at half-maximum (FWHM) of the (1 0 1) diffraction peak.

3.4 FTIR Spectral Analysis

FTIR spectral analysis of the pure TiO_2 and Ag-TiO_2 nanoparticles is illustrated in Fig. 4 (a and b). The spectral analysis confirmed that the silver ion behavior affects TiO_2 structure. A slight shift in several peaks can be ascribed to the binding effect of silver ions on anatase TiO_2 structure in Fig. 4b. The peaks that appeared at 650 cm^{-1} and 1352 cm^{-1} were due to the lattice vibrations

of TiO_2 structure, especially Ti-O-Ti Stretching mode of vibration (Fig. 4a). –OH bending and stretching modes were also observed at 1627cm^{-1} and 3380cm^{-1}, identifying the surface absorbed OH groups and water molecules (Li *et al.* 2005). Further, the addition of Ag on TiO_2 structural lattice, TiO_2 structural lattice vibration observed and shifted from 1400 cm^{-1} to 1335 cm$_{-1}$, which indicates the formation of bonding of Ag^+ ion in the lattice of TiO_2 structure. The band at 713 cm^{-1} can probably be due to Ti-O-Ag's asymmetric vibration (Tom *et al.*, 2003).

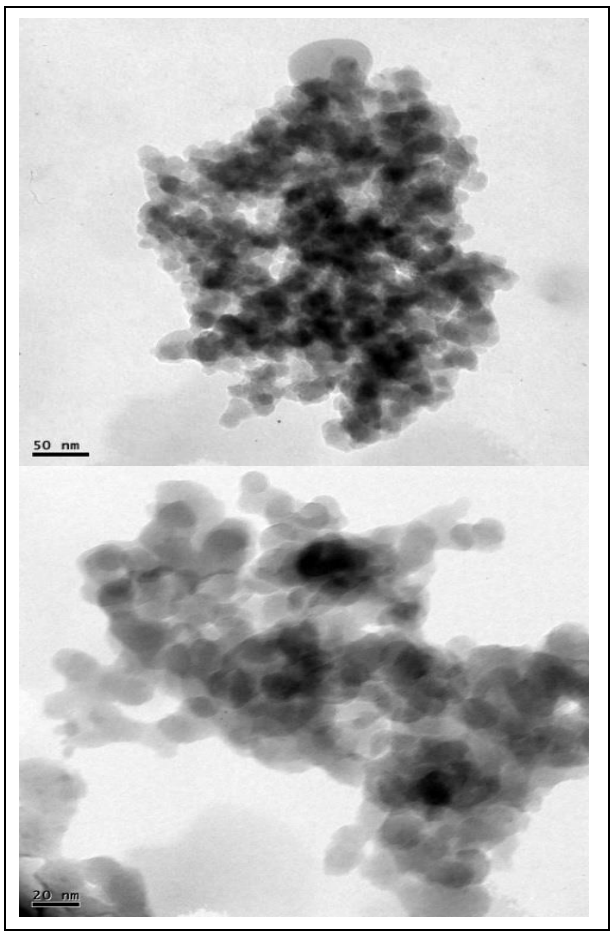

Fig. 2 (a, b) TEM analysis of pure TiO_2 and Ag-TiO_2 nanoparticles images with different magnification

3.5 UV-Visible Spectrum

UV-Visible spectral analysis of the pure TiO_2 and Ag-TiO_2 nanoparticles was illustrated in Fig. 5 (a and b). The figure shows absorbance at 320 nm and attained that bandgap of 3.26 eV, for TiO_2 and Ag-TiO_2 nanoparticles shows absorbance at 346 nm and attained that bandgap of 3.12 eV. The bandgap of TiO_2 shifted to the visible region because of Ag doping TiO_2. It has expected that redshift of the bandgap absorption expected while doping the silver ion on anatase phase TiO_2. Incorporation of silver in titanium oxide lattice has further profitability by the same route which has been utilized to boost the UV-Visible light reaping. Ag-TiO_2 nanoparticles have led to an effective photocatalytic degradation of methyl orange.

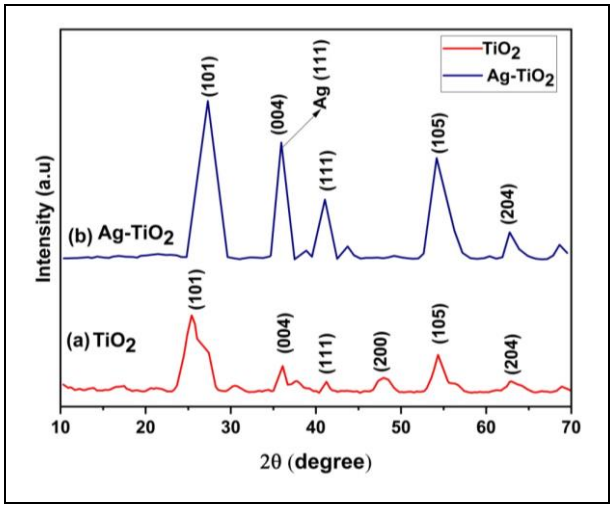

Fig. 3: XRD analysis of pure TiO_2 and Ag-TiO_2 samples

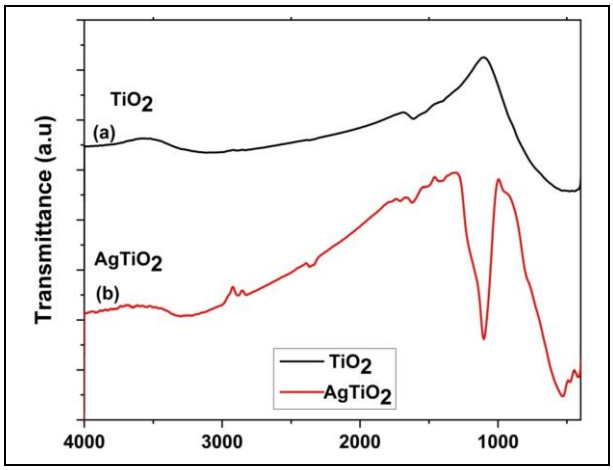

Fig. 4: FTIR analysis of pure TiO_2 and Ag-TiO_2 samples

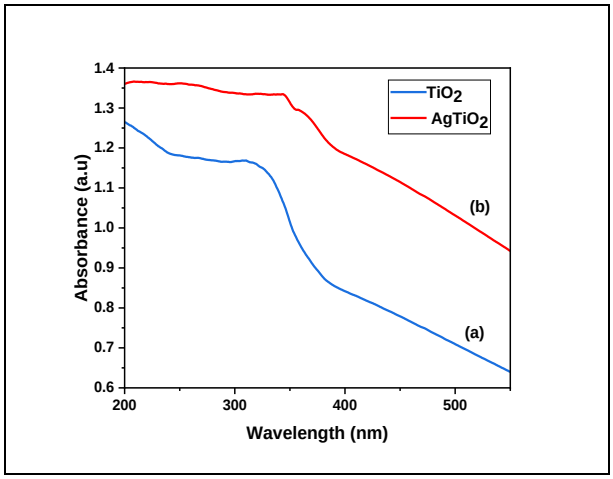

Fig. 5: UV-Visbile analysis of pure TiO_2 and Ag-TiO_2 samples

3.6 Determination of Surface Area - BET Method

The BET-specific surface areas of the samples calcined at 400₀C were 54 for TiO_2, and it gradually increases with increasing Ag concentration, and it was found to be 63 for Ag modified TiO_2, respectively. The characterization of Ag-modified TiO_2 materials has been reported elsewhere. The surface area of the TiO_2 increased as a result of Ag concentration. It is possible that Ag forms clusters within the TiO_2 nanoparticle sphere, thereby displacing some of the TiO_2 particles and increasing the surface area.

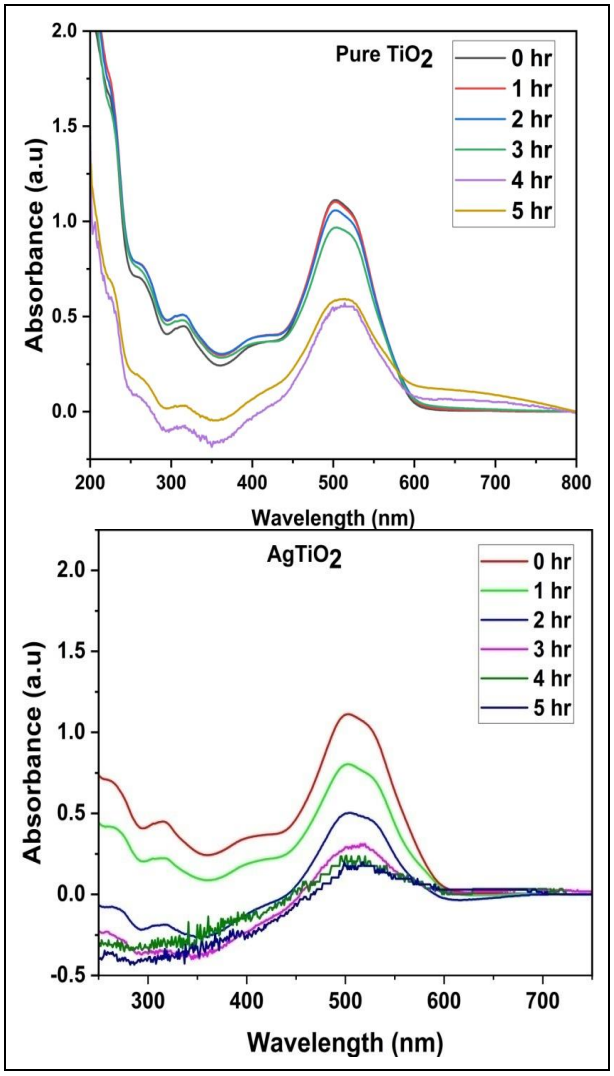

Fig. 6: Photocatalysis analysis of pure TiO_2 and Ag-TiO_2 samples at various time intervel

3.7 Photocatalyst Analysis

3.7.1 Results of Full-spectrum Scan

Fig. 6 shows the full spectrum scan of methyl orange within a 5 hours reaction at pH 9, dye concentration 50 mgL^{-1}, TiO_2 and Ag-TiO_2 concentration 10 mgL^{-1} with particle size 10 nm. The primary adsorption peaks of the original dye solution are 525 nm in the spectral range of 300 to 750 nm. As the reaction time increases, the peaks disappear gradually, and the full-spectrum scanning pattern changes after 5 hours. At the end of the 5 hr reaction time, no evident adsorption peak was observed at 525 nm. The adsorption also decreased. It indicates that the original chromophores in the dye solution are decomposed in the photocatalytic reaction and proves that methyl orange is decomposed in solar/TiO_2 and solar/Ag-TiO_2 systems.

3.8 Investigation on Biodegradability

COD of the water sample before and after decomposition was estimated by 0.1N $K_2Cr_2O_7$ solution. The COD level decreased from the initial concentration of 41.5 mg/L to 9.4 mg/L. The data indicate that the non-biodegradable organic part of the dye molecule was decomposed and mineralized in the photocatalytic process during the 5 hours reaction time. It has indicated that there were fewer organic compounds that were difficult to biodegrade after the decomposition of methyl orange.

4. CONCLUSION

TiO_2 nanoparticles (TiO_2) and Ag-doped TiO_2 nanocomposites (Ag-TiO_2) were synthesized by the Sol-Gel technique. The synthesized nanocomposites were characterized by XRD, SEM, TEM, FT-IR and UV-Visible analysis. The XRD results show that doping of Ag increases the grain size from 22 nm to 36 nm. Increasing grain size increases the bandgap and surface area, which shows good photocatalytic activity. The synthesized nanoparticles decompose the methyl orange dye within 5 hours.

FUNDING

This research received no specific grant from any funding agency in the public, commercial, or not-for-profit sectors.

CONFLICTS OF INTEREST

The authors declare that there is no conflict of interest.

REFERENCES

Abdul Gafoor, A. K., Musthafa, M. M., Pradyumnan, P. P., AC Conductivity and Diffuse Reflectance Studies of Ag-TiO_2 Nanoparticles, *J. Electron. Mater.* 41(9), 2387–2392 (2012). https://dx.doi.org/10.1007/s11664-012-2174-7

Almquist, C. B., Biswas, P., Role of Synthesis Method and Particle Size of Nanostructured TiO2 on Its Photoactivity, *J. Catal.* 212(2), 145–156 (2002). https://dx.doi.org/10.1006/jcat.2002.3783

Burns, A., Hayes, G., Li, W., Hirvonen, J., Demaree, J. D., Shah, S. I., Neodymium ion dopant effects on the phase transformation in sol–gel derived titania nanostructures, *Mater. Sci. Eng. B* 111(2–3), 150–155 (2004). https://dx.doi.org/10.1016/j.mseb.2004.04.008

Fox, M. A., Dulay, M. T., Heterogeneous photocatalysis, *Chem. Rev.* 93(1), 341–357 (1993). https://dx.doi.org/10.1021/cr00017a016

Fukuda, K., Nakai, I., Oishi, C., Nomura, M., Harada, M., Ebina, Y., Sasaki, T., Nanoarchitecture of Semiconductor Titania Nanosheets Revealed by Polarization-Dependent Total Reflection Fluorescence X-ray Absorption Fine Structure, *J. Phys. Chem. B* 108(35), 13088–13092 (2004). https://dx.doi.org/10.1021/jp047766w

Guo, H., Lin, K., Zheng, Z., Xiao, F., Li, S., Sulfanilic acid-modified P25 TiO2 nanoparticles with improved photocatalytic degradation on Congo red under visible light, *dye. Pigment.* 92(3), 1278–1284 (2012). https://dx.doi.org/10.1016/j.dyepig.2011.09.004

Jiang, B., Tian, C., Zhou, W., Wang, J., Xie, Y., Pan, Q., Ren, Z., Dong, Y., Fu, D., Han, J., Fu, H., In Situ Growth of TiO2 in Interlayers of Expanded Graphite for the Fabrication of TiO2-Graphene with Enhanced Photocatalytic Activity, *Chem. - A Eur. J.* 17(30), 8379–8387 (2011). https://dx.doi.org/10.1002/chem.201100250

Li, G., Li, L., Boerio-Goates, J., Woodfield, B. F., High Purity Anatase TiO 2 Nanocrystals: Near Room-Temperature Synthesis, Grain Growth Kinetics, and Surface Hydration Chemistry, *J. Am. Chem. Soc.* 127(24), 8659–8666 (2005). https://dx.doi.org/10.1021/ja050517g

Liu, S., Yu, J., Jaroniec, M., Tunable Photocatalytic Selectivity of Hollow TiO 2 Microspheres Composed of Anatase Polyhedra with Exposed {001} Facets, *J. Am. Chem. Soc.* 132(34), 11914–11916 (2010). https://dx.doi.org/10.1021/ja105283s

Rajamanickam, D., Dhatshanamurthi, P., Shanthi, M., Enhanced photocatalytic efficiency of NiS/TiO2 composite catalysts using sunset yellow, an azo dye under day light illumination, *Mater. Res. Bull.* 61, 439–447 (2015). https://dx.doi.org/10.1016/j.materresbull.2014.09.095

Sahu, M., Wu, B., Zhu, L., Jacobson, C., Wang, W.-N., Jones, K., Goyal, Y., Tang, Y. J., Biswas, P., Role of dopant concentration, crystal phase and particle size on microbial inactivation of Cu-doped TiO_2 nanoparticles, *Nanotechnol.*, 22(41), 415704 (2011). https://dx.doi.org/10.1088/0957-4484/22/41/415704

Tom, R. T., Nair, A. S., Singh, N., Aslam, M., Nagendra, C. L., Philip, R., Vijayamohanan, K., Pradeep, T., Freely Dispersible Au@TiO_2, Au@ZrO_2, Ag@TiO_2, and Ag@ZrO_2 Core−Shell Nanoparticles: One-Step Synthesis, Characterization, Spectroscopy, and Optical Limiting Properties, *Langmuir*, 19(8), 3439–3445 (2003). https://dx.doi.org/10.1021/la0266435

Wang, Y., Du, G., Liu, H., Liu, D., Qin, S., Wang, N., Hu, C., Tao, X., Jiao, J., Wang, J., Wang, Z. L., Nanostructured Sheets of TiO Nanobelts for Gas Sensing and Antibacterial Applications, *Adv. Funct. Mater.*, 18(7), 1131–1137 (2008). https://dx.doi.org/10.1002/adfm.200701120